Increased intramyocellular lipid content but normal skeletal muscle mitochondrial oxidative capacity throughout the pathogenesis of type 2 diabetes.

Increased intramyocellular lipid content but normal skeletal muscle mitochondrial oxidative capacity throughout the pathogenesis of type 2 diabetes

Henk M. De Feyter,*[,1] Ellen Lenaers,[†] Sander M. Houten,[§] Patrick Schrauwen,[‡] Matthijs K. Hesselink,[†] Ronald J. A. Wanders,[§] Klaas Nicolay,* and Jeanine J. Prompers*

*Biomedical NMR, Department of Biomedical Engineering, Eindhoven University of Technology, Eindhoven, The Netherlands; [†]Department of Human Movement Sciences and [‡]Department of Human Biology, Nutrition and Toxicology Research Institute Maastricht, Maastricht University, Maastricht, The Netherlands; and [§]Department of Clinical Chemistry, Laboratory Genetic Metabolic Diseases, Academic Medical Center, Amsterdam, The Netherlands

ABSTRACT **Currently inherited or acquired skeletal muscle mitochondrial dysfunction is linked to dysregulated fatty acid metabolism, resulting in increased levels of intramyocellular lipids (IMCLs) and lipid intermediates, inducing insulin resistance. The present study aimed to clarify the order of changes in IMCL levels and skeletal muscle mitochondrial function during the development of type 2 diabetes in Zucker diabetic fatty (ZDF) rats. IMCL levels and skeletal muscle oxidative capacity were determined *in vivo*, using localized ^{1}H magnetic resonance spectroscopy (MRS) and dynamic ^{31}P MRS, respectively. In parallel, *in vitro* activities were measured from enzymes involved in fatty acid oxidation, the tricarboxylic acid cycle and the electron transport chain. Fa/fa ZDF rats were studied at 3 different ages corresponding to different stages of type 2 diabetes, whereas fa/+ rats served as controls. Fa/fa ZDF rats had higher IMCL contents than controls throughout the duration of the study. *In vivo* muscle oxidative capacity was not different in fa/fa animals compared to controls, and *in vitro* enzyme activity data suggested improved functionality of enzymes involved in fat oxidation in type 2 diabetic animals. Accordingly, we can conclude that in the ZDF rat model, type 2 diabetes develops in the absence of skeletal muscle mitochondrial dysfunction.—De Feyter, H. M., Lenaers, E., Houten, S. M., Schrauwen, P., Hesselink, M. K., Wanders, R. J. A., Nicolay, K., Prompers, J. J. Increased intramyocellular lipid content but normal skeletal muscle mitochondrial oxidative capacity throughout the pathogenesis of type 2 diabetes. *FASEB J.* 22, 3947–3955 (2008)**

Key Words: rat · NMR spectroscopy · In vivo NMR · insulin resistance · PCr recovery

Skeletal muscle accounts for the great majority of insulin-stimulated glucose uptake (1), and insulin resistance of skeletal muscle tissue is one of the earliest detectable disturbances in the development of type 2 diabetes [reviewed by Petersen and Shulman (2)]. It has been shown that insulin sensitivity is negatively correlated with the amount of intramyocellular lipids (IMCLs) stored inside skeletal muscle cells. This relationship has been described in sedentary humans (3–6) as well as in rat models of insulin resistance and type 2 diabetes (7–9). A causal relationship between IMCL accumulation and insulin resistance has never been demonstrated, but there are strong indications that intermediates of lipid metabolism, such as long-chain acyl-CoAs, diacylglycerol, and/or ceramides impede the insulin signaling rather than the stored triglycerides themselves (10, 11).

Recently, insulin resistance has also been associated with skeletal muscle mitochondrial dysfunction (12, 13). Data originating from *in vivo* magnetic resonance spectroscopy (MRS) measurements (14–17), *in vitro* enzyme activity assays (18–21), and expression analysis of genes involved in oxidative metabolism (22, 23) suggest that skeletal muscle mitochondrial dysfunction plays a role in insulin resistance and type 2 diabetes. Current hypotheses link inherited or acquired mitochondrial dysfunction to impaired fatty acid metabolism, which subsequently results in increased levels of IMCLs and lipid intermediates, inducing insulin resistance (2, 13–15, 24).

Studies in humans investigating the relations among mitochondrial function, IMCLs, and insulin resistance or type 2 diabetes have been carried out using cross-sectional study designs. Because these studies only provide correlative information, it is impossible to unravel cause and consequence. In an attempt to bypass these limitations, we studied an established animal model of type 2 diabetes, the Zucker diabetic fatty (ZDF) rat, aiming to

[1] Correspondence and current address: Yale University, MRRC, TAC N 136, 300 Cedar St., PO Box 208043, New Haven, CT 06520-8043, USA. E-mail: henk.defeyter@yale.edu

doi: 10.1096/fj.08-112318

clarify the order in which changes in IMCLs and *in vivo* skeletal muscle mitochondrial function occur during the development of type 2 diabetes. Localized ^{1}H MRS was used to determine IMCL content, and dynamic ^{31}P MRS was applied in combination with a minimally invasive electrical stimulation method to measure post-exercise resynthesis kinetics of phosphocreatine (PCr). The postexercise PCr recovery time constant provides a measure of *in vivo* muscle oxidative capacity because the muscle contractions create a highly activated state of the mitochondria (*i.e.*, high ADP levels) and ATP used to restore the PCr pool during recovery is originating exclusively from mitochondrial oxidative phosphorylation (25).

Fa/fa ZDF rats were studied *in vivo* in a longitudinal study design at ages corresponding to *1*) a normoglycemic-hyperinsulinemic state (prediabetic), *2*) a hyperglycemic-hyperinsulinemic state (overt type 2 diabetes), and *3*) a late type 2 diabetes stage characterized by hyperglycemia and progressive β-cell failure (26). Heterozygous fa/+ rats remain normoglycemic and normoinsulinemic and served as controls (26). In addition, muscle tissue was collected from parallel groups of animals at the same time points as the *in vivo* MRS measurements to measure *in vitro* activities of enzymes/complexes of β-oxidation, tricarboxylic acid (TCA) -cycle, and electron transport chain (ETC) in homogenized muscle samples.

Based on phenotypical characteristics of fa/fa rats, we hypothesized that the development of overt type 2 diabetes in fa/fa rats would be paralleled by a progressive loss of *in vivo* mitochondrial oxidative capacity and increase in IMCL content compared to the control fa/+ rats. Similarly, *in vitro* enzyme activities were expected to progressively decrease in fa/fa rats with advancing type 2 diabetes.

MATERIALS AND METHODS

Animals

Male obese ZDF rats (ZDF/Gmi, fa/fa; n=22) and lean littermates (ZDF/Gmi, fa/+; n=23) (Charles River Laboratories, The Netherlands) were housed in pairs at 20°C and 50% humidity, on a 12-h light-dark cycle with *ad libitum* access to water and chow during the entire study. Animals arrived at the laboratory at 5 wk of age. From 7 wk of age, animals received a diet containing, as percentage of calories, 16.7% fat, 56.4% carbohydrates and 26.8% protein (Altromin, Lage, Germany). Body weight and food intake were monitored weekly. Principles of laboratory animal care were followed and all experimental procedures were approved by the Animal Ethics Committee of Maastricht University.

MRS groups

In 10 fa/fa and 11 fa/+ animals, IMCL levels and skeletal muscle oxidative capacity were measured in tibialis anterior (TA) muscle by applying *in vivo* ^{1}H and ^{31}P MRS, respectively, at 6, 12, and 18 wk of age. In the week after the last MRS experiments (19 wk of age), the animals were killed and muscle tissue was harvested according to procedures described for the parallel groups.

Parallel groups

Parallel to the MRS measurements, ZDF rats were killed at 6 (fa/fa, n=6; fa/+, n=6) and 12 (fa/fa, n=6; fa/+, n=6) wk of age by cervical dislocation within 20 s following CO_2 sedation. TA muscles were excised, and midbelly portions were rapidly frozen in liquid nitrogen and stored at −80°C.

MRS

All MRS measurements were performed on a 6.3 T horizontal Bruker MR system (Bruker, Ettlingen, Germany). During preparatory surgical procedures and MRS experiments, animals were anesthetized using 1–2% isoflurane (Forene; Abbot GmbH, Wiesbaden, Germany) administered *via* a face mask with medical air (0.4 L/min), and body temperature was maintained at 37 ± 1°C using heating pads. In the MR scanner, respiration was monitored using a pressure sensor registering thorax movement (Rapid Biomedical, Rimpar, Germany).

Single-voxel localized ^{1}H MRS was applied to measure IMCL levels in TA, as described elsewhere (27) except that no additional outer volume suppression was used. In short, 2 voxels of $2 \times 2 \times 2$ mm^3 were subsequently measured in white (ventral) and red (dorsal) TA, respectively, using an ellipsoid ^{1}H surface coil (18/22 mm). The ^{1}H MR spectra were acquired using the LASER (localization by adiabatic selective refocusing) sequence (28) [repetition time TR=1 s, echo time TE=16 ms, SWAMP (sequence for water suppression with adiabatic modulated pulses) water suppression (29), 512 averages].

^{31}P MRS was applied using a combination of a circular ^{1}H surface coil (40 mm) and an ellipsoid ^{31}P surface coil (10/18 mm) positioned over the TA. Localized shimming was performed on the water signal using the ^{1}H surface coil. ^{31}P spectra were acquired applying an adiabatic excitation pulse with a flip angle of 90°. A fully relaxed spectrum (TR=20 s, 32 averages) and a partially saturated spectrum (TR=5 s, 128 averages) were measured at rest, followed by the acquisition of a time series of spectra (TR=5 s, 4 averages) before, during, and after electrical stimulation of TA. Electrical stimulation was applied *via* acute, subcutaneously implanted platinum electrodes positioned along the distal nerve trajectory of the n. peroneus communis to induce contractions in the TA. A time series consisted of 3 min rest, 2 min of electrical stimulation, and 10 min of recovery. Stimulation pulse length was 100 ms, frequency was 80 Hz, stimulation voltage varied between 2 and 4 V, and pulses were applied 1/s. For each rat, at each age at least 3 consecutive time series were performed. During the first time series, stimulation voltage was adjusted to assure significant depletion of PCr in subsequent time series. The latter 2 time series were used for analysis of PCr recovery kinetics.

Both ^{31}P and ^{1}H MR spectra were fit in the time domain by using a nonlinear least squares algorithm in the jMRUI software package (30). ^{1}H MR spectra were fit as described elsewhere (27). IMCL was then expressed relative to total creatine (tCr). For the ^{31}P MR spectra recorded at rest, PCr and the intra- and extracellular inorganic phosphate (Pi) peaks (31) were fit to Lorentzian line shapes. The α- and γ-ATP peaks were fit to Gaussian line shapes with equal peak areas. Due to limited bandwidth of the excitation pulse, the β-ATP had lower amplitude and was not fit. In ^{31}P MR spectra from the time series, peaks from intra- and extracellular Pi could not be distinguished; therefore, a single Pi peak was fit

to a Gaussian line shape. Absolute concentrations of the phosphorylated metabolites were calculated after correction for partial saturation with the assumption that the ATP concentration is 8.2 mM at rest (32). Intracellular pH was calculated from the chemical shift difference between the Pi and PCr resonances (33). The free cytosolic ADP concentration was calculated from the PCr concentration and pH using a creatine kinase equilibrium constant (K_{eq}) of 1.66×10^9 M^{-1} (34) and the assumption that 15% of the total creatine is unphosphorylated at rest (35). For the time series, the PCr line width during recovery was constrained to the average PCr line width during recovery (excluding the first 5 data points) obtained from a prior, unconstrained fit. The data of PCr resynthesis were fit to a monoexponential function using Matlab (version 6.5, Mathworks, Natick, MA, USA) yielding a time constant τ_{PCr}, which is a measure of skeletal muscle mitochondrial oxidative capacity. Two time series with similar end-exercise pH values were analyzed for each animal, resulting in 2 values of τ_{PCr}, which were averaged.

In vitro enzyme activities

Muscle tissue (frozen microtome section) was disrupted using sonication (twice at 8-W output, 40 J, on ice) in homogenization buffer (50 mM Tris, 120 mM NaCl, 5mM KCl, 1 mM $MgSO_4$, 1 mM $CaCl_2$, and 10% glycerol, pH 7.4). The homogenates were centrifuged for 5 min at 1000 *g*. Protein concentration was determined in the supernatant using the Bradford method. The homogenates were diluted to ~1 mg/mL. Very long chain acyl-CoA dehydrogenase (VLCAD) activity was measured as described elsewhere, using palmitoyl-CoA as substrate (36). The production of trans-2,3-palmitoyl-CoA and L-3-hydroxypalmitoyl-CoA was quantified by HPLC and used to calculate acyl-CoA dehydrogenase activity. Citrate synthase (CS) was measured spectrophotometrically at 412 nm by the formation of free CoA using 5,5′-dithio-bis-(2-nitrobenzoic acid) (37). Succinate dehydrogenase (SDH) was measured using a method described by Munujos *et al.* (38). Cytochrome *c* oxidase (complex IV) activity was measured by following the formation of oxidized cytochrome *c* at 550 nm using a method described by Cooperstein and Lazarow (39).

Plasma parameters

Blood samples were collected from animals *via* the retro-orbital plexus at 6, 12, and 18 wk of age, under isoflurane anesthesia, after 4 h of food deprivation (randomly $n=6$/genotype). The blood samples were collected in K-EDTA coated tubes and centrifuged for 10 min at 1000 *g*, and plasma aliquots were frozen in liquid nitrogen and stored at −80°C. Plasma glucose content was determined using the hexokinase method (Roche, Basel, Switzerland), and free fatty acids (FFAs) were measured with the Wako NEFA C test kit (Wako Chemicals, Neuss, Germany). Fasting plasma insulin concentrations were determined using an ultrasensitive solid phase two-site ELISA kit (Mercodia, Uppsala, Sweden).

Statistical analysis

Data are presented as means ± SD. MRS data were analyzed using ANOVA for repeated measures with 1 within-subjects factor (age) and 1 between-subjects factor (genotype). Bonferroni corrected *post hoc* tests were carried out in order to identify differences between different ages. Two-way ANOVA was used to analyze the metabolic plasma parameters and the *in vitro* enzyme activities. When there was a significant effect of the interaction term age × genotype, data were analyzed again using the relevant ANOVA for each genotype separately to detect effects of age. Independent sample *t* tests were used at different ages to detect differences between genotypes. All tests were performed two-sided using SPSS 14.0 (SPSS Inc, Chicago, IL, USA), and statistical significance was set at $P \leq 0.05$.

RESULTS

Animal model

Body weight was higher in fa/fa than in fa/+ rats during the entire study ($P<0.001$ at every time point). Fa/fa rats had a higher body weight at the start of the study and appeared to increase in body weight at a higher rate than fa/+ animals between week 6 and 11. *Ad libitum* food intake of fa/fa rats was higher than that of fa/+ rats over the entire study duration ($P<0.001$ at every time point).

Plasma concentrations of glucose, insulin, and FFAs determined at 6, 12, and 18 wk of age are depicted in **Fig. 1**. For both glucose and insulin, there was a significant age × genotype interaction ($P<0.001$ and $P=0.04$, respectively), which was attributable to the age-related changes in fa/fa rats. Fa/+ animals displayed normal and constant glucose and insulin levels throughout the entire study (Fig. 1*a*, *b*). At all ages, the glucose and insulin levels were significantly higher in

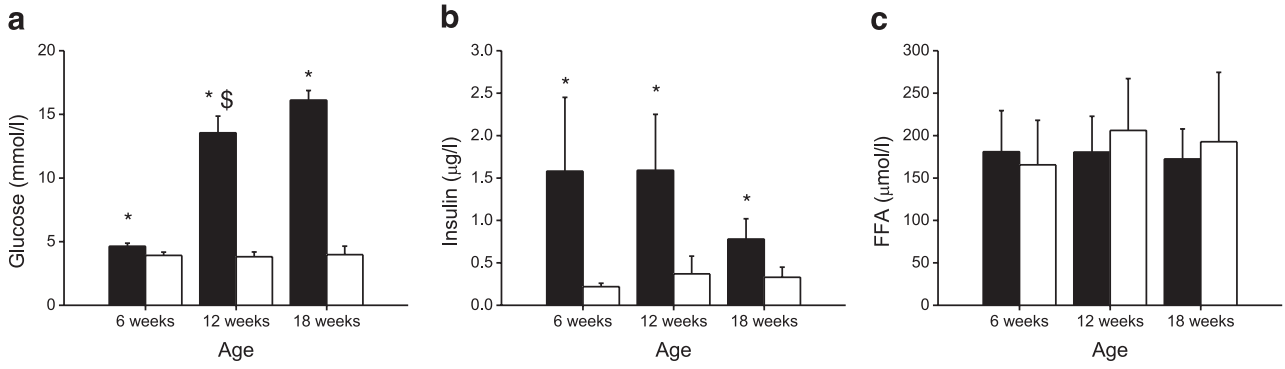

Figure 1. Fasting plasma concentrations of glucose (*a*), insulin (*b*), and FFA (*c*) at 6, 12, and 18 wk of age. Filled bars, fa/fa rats; open bars, fa/+ rats. $^*P < 0.05$ *vs.* fa/+ rats of the same age; $^\$P < 0.05$ *vs.* 6- and 18-wk-old fa/fa rats. Error bars represent SD.

fa/fa rats compared to controls ($P<0.001$ for glucose and $P<0.05$ for insulin). The plasma data confirm that at 6 wk of age, fa/fa animals were euglycemic-hyperinsulinemic (prediabetic); at 12 wk, fa/fa animals were diabetic, displaying hyperglycemia and hyperinsulinemia; and at 18 wk, they were in an advanced diabetic state, with hyperglycemia but decreased insulin levels compared to 12 wk. Both genotypes showed similar and constant plasma FFA levels during the period of the study (Fig. 1*c*).

IMCLs

Figure 2*a*, *b* shows representative examples of ^{1}H MR spectra measured in red TA of a fa/fa and a fa/+ rat, respectively, at the age of 12 wk. The spectra clearly depict the increased amplitude of the IMCL resonances measured in the fa/fa rat compared to the control fa/+ rat. The mean IMCL levels at different ages for white and red regions of the TA muscle are presented in Fig. 2*c*, *d*, respectively. In both genotypes and at all ages, IMCL levels were ~2–3 times higher in the red region of the TA compared to the white region. There was a significant age × genotype interaction effect for IMCLs in both red and white regions of the TA muscle. Analyzing the age effect on IMCL levels within each genotype separately showed a trend toward a decrease ($P=0.077$) in white TA and a significant decrease in red TA ($P<0.01$) of fa/+ animals. In contrast, IMCL levels significantly increased in fa/fa rats between 6 and 12 wk of age (red and white TA, both $P<0.01$), and decreased again between 12 and 18 wk of age in white TA ($P=0.012$), and tended to decrease in red TA ($P=0.09$). IMCL levels were significantly higher in fa/fa rats compared to fa/+ animals for both the white and red region of the TA at all ages (all $P<0.05$). Compared to the euglycemic-hyperinsulinemic state (6 wk of age), the difference in IMCL content was amplified in the hyperglycemic-hyperinsulinemic state (12 wk of age), and IMCL levels remained much higher in fa/fa rats compared to fa/+ animals in the advanced diabetic state.

^{31}P MRS

Table 1 lists the ^{31}P metabolite concentrations and pH at rest. The intracellular Pi concentration [Pi] and [Pi]/[PCr] was higher in fa/fa rats than in fa/+ rats (both $P<0.001$) at all time points. Both parameters were changing during maturation in both genotypes: [Pi] increased between 12 and 18 wk of age ($P<0.001$), and [Pi]/[PCr] decreased between 6 and 12 wk of age ($P=0.023$), but increased again between 12 and 18 wk of age ($P<0.001$). There was also an effect of aging in both genotypes on [PCr], [ADP], and pH, which all increased from 6 to 12 wk of age ([PCr] and [ADP]: $P<0.001$; pH: $P=0.001$), but remained constant during further maturation.

Figure 3*a* shows a stack plot of spectra measured during a rest-exercise-recovery protocol and demonstrates how the PCr signal drops when the electrical stimulation starts, reaches a steady state, and then recovers when ceasing stimulation. End-exercise metabolite concentrations and pH are presented in **Table 2**.

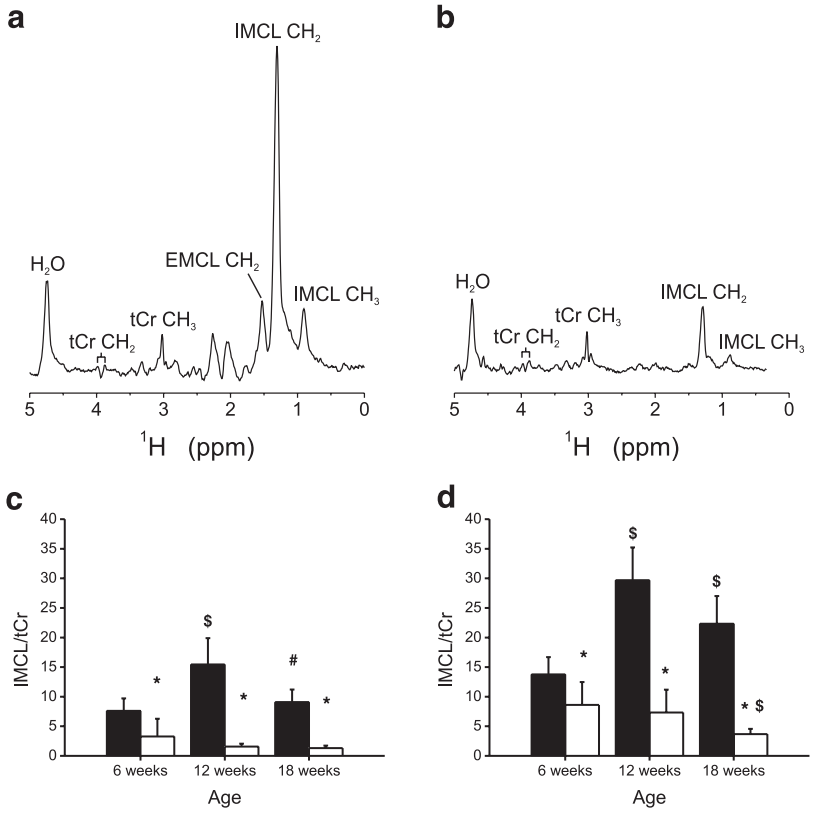

Figure 2. Examples of water-suppressed ^{1}H MR spectra measured in red TA from a 12-wk-old fa/fa (*a*) and fa/+ (*b*) rat. Peak annotations: H_2O, residual water; EMCL, extramyocellular lipids. IMCL content at different ages in white (*c*) and red TA (*d*). Filled bars, fa/fa rats; open bars, fa/+ rats. $^*P < 0.05$ *vs.* fa/fa rats of the same age; $^{\$}P < 0.05$ *vs.* 6-wk-old rats of same genotype; $^{\#}P < 0.05$ *vs.* 12-wk-old fa/fa rats. Error bars represent SD.

TABLE 1. *Concentrations of ^{31}P metabolites and intracellular pH at rest*

	6 wk		12 wk		18 wk	
Measure	fa/fa	fa/+	fa/fa	fa/+	fa/fa	fa/+
[PCr] (mM)	31.7 ± 1.2	32.5 ± 1.5	40.2 ± 1.2[b]	38.5 ± 1.0[b]	39.1 ± 2.0[b]	39.5 ± 1.6[b]
[Pi] (mM)[a]	3.2 ± 0.7	2.5 ± 0.6	3.1 ± 0.7	2.3 ± 0.5	4.3 ± 0.6[c]	3.3 ± 0.6[c]
[Pi]/[PCr][a]	0.1 ± 0.02	0.08 ± 0.02	0.08 ± 0.02[b]	0.06 ± 0.01[b]	0.11 ± 0.02[c]	0.08 ± 0.02[c]
[ADP] (μM)	9.6 ± 1.6	9.9 ± 1.6	12.0 ± 0.4[b]	11.4 ± 0.5[b]	11.3 ± 0.5	11.7 ± 0.7
pH	7.04 ± 0.08	7.05 ± 0.07	7.14 ± 0.02[b]	7.12 ± 0.02[b]	7.11 ± 0.02	7.13 ± 0.03

[a] Significantly different between genotypes. [b] Significantly different compared to 6-wk-old animals. [c] Significantly different compared to 12-wk-old animals.

End-exercise [Pi] was higher in fa/fa than in fa/+ animals. The other metabolite's concentrations were similar in both genotypes. End-exercise [PCr], [ADP], and pH were higher at 12 wk compared to 6 wk of age, which can most probably be attributed to the applied electrical stimulation protocol. At 12 wk of age, (erroneously) slightly less strenuous contractions were induced, explaining the differences in end-exercise [PCr], [ADP], and pH. At each age, however, end-exercise pH did not differ between genotypes.

Figure 3*b* depicts an example of the PCr recovery fit. The mean R^2 for the fit procedure of the individual recovery datasets was 0.96 ± 0.03. The mean PCr recovery time constants of both genotypes at different ages are depicted in Fig. 3*c*. Repeated-measures ANOVA revealed no significant effect of genotype or genotype × age on τ_{PCr}. However, in both genotypes, there was a significant effect of age; that is, at 12 wk τ_{PCr} was greater than at 6 wk, and at 18 wk τ_{PCr} was greater than at 12 wk (all $P<0.001$), indicating a significant decrease in muscle *in vivo* oxidative capacity with aging.

In vitro enzyme assays

We measured activities of VLCAD (**Fig. 4*a***), CS (Fig. 4*b*), SDH (Fig. 4*c*), and complex IV (Fig. 4*d*) in the different ZDF genotypes at different ages in order to evaluate mitochondrial function *in vitro*. The statistical analysis of VLCAD activities revealed a borderline significance ($P=0.06$) for the interaction of age and genotype and a significant effect of genotype ($P=0.001$): higher VLCAD activities were measured in fa/fa animals compared to fa/+ rats at 12 and 19 wk of age (Fig. 4*a*). CS activities displayed a significant genotype effect ($P=0.045$) in the ANOVA, which became weaker in the *post hoc* comparisons: at 19 wk of age, fa/fa rats showed a trend for higher CS activity compared to fa/+ rats ($P=0.075$) (Fig. 4*b*). SDH enzyme activities did not differ between genotypes and also remained unchanged with age (Fig. 4*c*). The statistical analysis of complex IV activities illustrated a significant effect of both genotype and age. Complex IV activity was higher in 6-wk-old fa/fa rats compared to control rats (Fig. 4*d*). Complex IV activity decreased in both genotypes, but to a lesser extent in fa/fa rats, resulting in higher enzyme activity in 19-wk-old fa/fa rats compared to controls.

DISCUSSION

The present study aimed to clarify the order in which changes in IMCL content and skeletal muscle mito-

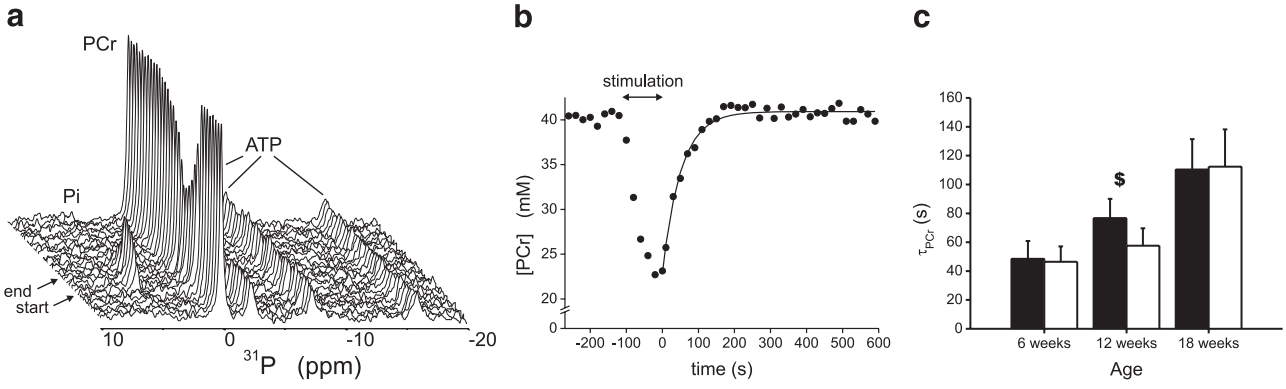

Figure 3. *a*) Stack plot of ^{31}P MR spectra measured in TA during a time series of a 12-wk-old fa/+ rat during a rest-exercise-recovery protocol. Contractions were induced by electrical stimulation. The period of electrical stimulation (2 min) is indicated with the arrows (start and stop). Time resolution=20 s. Peaks are from Pi, PCr, and ATP. *b*) [PCr] during rest-exercise-recovery protocol. Recovery data were fit with a monoexponential function (black line); $\tau_{PCr}=51.1$ s. *c*) Average τ_{PCr} of fa/fa (filled bars) and fa/+ rats (open bars) at different ages. A higher value of τ_{PCr} indicates a lower oxidative capacity. $^{\$}P<0.05$ *vs.* 6- and 18-wk-old rats. Error bars represent SD.

TABLE 2. *Concentrations of ^{31}P metabolites and intracellular pH at the end of exercise*

	6 wk		12 wk		18 wk	
Measure	fa/fa	fa/+	fa/fa	fa/+	fa/fa	fa/+
[PCr] (mM)	16.7 ± 2.3	17.0 ± 2.3	21.4 ± 2.3[b]	19.9 ± 2.0[b]	19.5 ± 1.7[b]	21.8 ± 1.6[b]
[Pi] (mM)[a]	21.1 ± 3.7	17.7 ± 1.8	20.5 ± 3.7	15.8 ± 2.4	22.5 ± 4.4	17.6 ± 2.9
[ADP] (μM)	47.3 ± 16.4	53.4 ± 19.3	57.9 ± 9.06[b]	67.2 ± 9.8[b]	59.2 ± 13.0	51.3 ± 10.9
pH	6.86 ± 0.11	6.91 ± 0.07	6.98 ± 0.08[b]	7.02 ± 0.10[b]	6.93 ± 0.02	6.96 ± 0.06

[a] Significantly different between genotypes. [b] Significantly different compared to 6-wk-old animals.

chondrial function occur during the development of type 2 diabetes in ZDF rats. We hypothesized that *in vivo* mitochondrial oxidative capacity and *in vitro* activities of enzymes involved in oxidative metabolism would show a progressive decrease parallel to the development of type 2 diabetes. Furthermore, IMCL levels were expected to increase during the development of type 2 diabetes. IMCL levels were higher in prediabetic fa/fa rats than in controls and increased in fa/fa rats with the development of type 2 diabetes. Although IMCL content did not continue to rise between 12 and 18 wk of age, IMCL levels were always higher in fa/fa rats compared to control animals. In agreement with our hypothesis, *in vivo* mitochondrial oxidative capacity progressively decreased throughout the duration of the study, as evidenced by the increased time constant for PCr recovery after exercise. However, since this occurred to a similar degree in both ZDF genotypes, the decreased oxidative capacity did not seem to play a major role in the development of type 2 diabetes in the fa/fa rats. In accordance with the *in vivo* measurements, *in vitro* enzyme activities were not decreased in fa/fa rats compared to control animals at any age. VLCAD and complex IV activities were even higher, and CS activity tended to be higher in late-stage diabetic fa/fa rats than in control fa/+ rats.

The *in vivo* IMCL measurements confirm previous results on muscle fiber type-related levels of IMCLs within Wistar rat TA muscle (27), as in both ZDF genotypes IMCL levels were 2–3 times higher in red TA compared to white TA. Relative changes in IMCL levels during the study were similar in white and red TA, both in fa/fa and in fa/+ rats. In general, the age-dependent changes in IMCL content of ZDF rats are in good agreement with earlier reports (8).

At 6 wk of age, *in vivo* skeletal muscle oxidative capacity was identical in both genotypes despite the hyperinsulinemic state of fa/fa rats. This implies that hyperinsulinemia develops without skeletal muscle mitochondrial dysfunction in the 6-wk-old fa/fa rats. During the transition from the normoglycemic-hyperinsulinemic state toward the hyperglycemic-hyperinsulinemic state, τ_{PCr} in fa/fa rats gradually increased, resulting in about 3 times higher values at 18 wk compared to 6 wk of age. However, a similar change in τ_{PCr} was observed in maturing normoglycemic-normoinsulinemic fa/+ rats. Therefore, this decrease in oxidative capacity can most likely be entirely attributed to

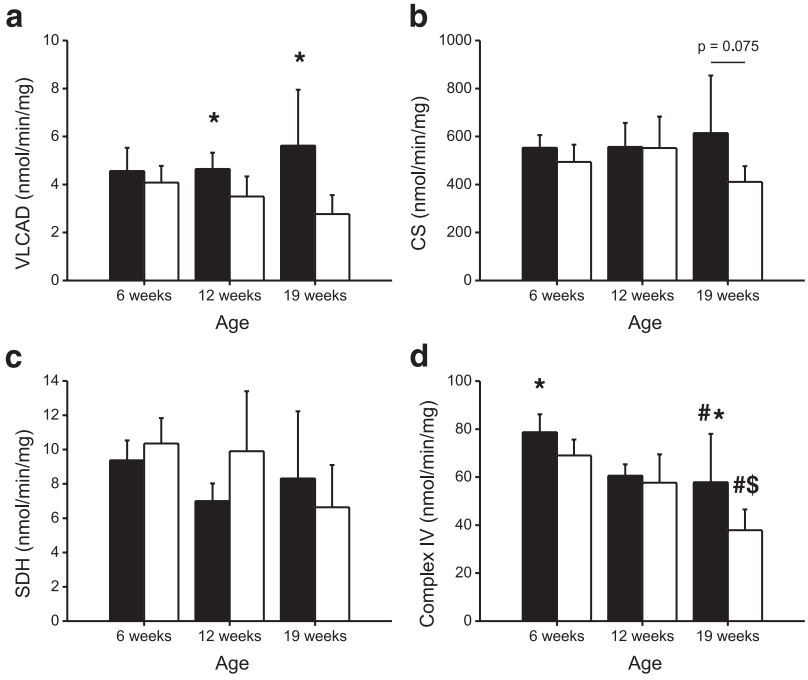

Figure 4. Activities of VLCAD (*a*), CS (*b*), SDH (*c*), and complex IV (*d*) in the different ZDF genotypes at different ages. Activities were determined in 6 animals/group. *$P<0.05$ *vs.* fa/+ rats of the same age; #$P<0.05$ *vs.* 6-wk-old animals of same genotype; $$P<0.05$ *vs.* 12-wk-old animals of same genotype. Error bars represent SD.

aging of the animals. Healthy Wistar rats display a similar degree of age-related decrease in oxidative capacity, and τ_{PCr} values of the TA are similar to those measured in ZDF rats (data not shown). Thus, our data do not reveal apparent mitochondrial dysfunction in the diabetic ZDF phenotype. On the other hand, we cannot completely exclude that the combination of both the age-related decrease of *in vivo* mitochondrial oxidative capacity and high IMCL levels contributed to the development of type 2 diabetes.

Sanderson *et al.* (40) measured PCr recovery kinetics in 15-wk-old, obese, insulin-resistant Zucker rats. There were no differences observed in τ_{PCr} between obese Zucker rats and lean controls; CS activities were also the same (40). In contrast, Klein *et al.* (41) reported slower postexercise recovery of PCr in obese Zucker rats compared to lean controls. However, their ^{31}P MR spectra were recorded with relatively low time resolution (2 min), which impeded a robust quantitative analysis of the recovery data. Furthermore, the end-exercise pH was significantly lower in the obese animals, which does not allow comparison of the PCr recovery rates between both animal groups, as was also argued by the authors (41).

To study diet-induced alterations in skeletal muscle mitochondrial function, Chanseaume *et al.* (42) fed Wistar rats a high-fat diet and sacrificed them at sequential time points. Measuring *in vitro* mitochondrial respiration and ATP production in skinned muscle fibers, they found no differences in the TA muscle of Wistar rats fed a high-fat diet compared with control animals, which is in agreement with our results. However, in a later stage, after 40 days of consuming a high-fat diet, the soleus muscle showed a decrease in oxidative phosphorylation activity (42). In young Wistar rats fed a high-fat diet for 15 days, increased lipid oxidative capacity was measured in muscle homogenates and subsarcolemmal and intermyofibrillar mitochondria (43). More recently, however, the same group showed that a longer period (7 wk) of high-fat diet consumption in adult rats resulted in a lower respiratory capacity of subsarcolemmal mitochondria (44). The duration of the diet and the age of the animals at the start of the intervention have been proposed as factors accountable for these different results in Wistar rats (44, 45). In diet-induced insulin-resistant mice, skeletal muscle mitochondrial function was not affected after 4 wk of diet. However, after 16 wk of high-fat and high-sucrose diet, reactive oxygen species (ROS) induced mitochondrial dysfunction (46). The data from these diet-induced diabetic mice suggest that mitochondrial alterations do not precede insulin resistance and result from increased ROS production in muscle (46). Although we have studied relatively long-term effects of insulin resistance and type 2 diabetes, we cannot exclude that at older age, a decreased *in vivo* oxidative capacity might develop in fa/fa rats secondary to longer exposure to overt type 2 diabetes.

Although PCr recovery analysis provides an excellent measure of *in vivo* mitochondrial oxidative capacity in general, it does not offer information about the pattern of substrates utilized by the mitochondrial respiratory chain. Keeping in mind the short duration of the muscle contraction protocol, it is fair to assume that the oxidative phosphorylation during contraction and recovery relies predominantly on carbohydrates as a fuel. Differences in fat oxidative capacity that do not lead to a general dysfunction of the mitochondria will therefore remain undetected in postexercise PCr recovery analysis. However, *in vitro* VLCAD activity did not show an impairment in fa/fa animals, either. Rather, the opposite occurred, as we observed a significant up-regulation of VCLAD activity in fa/fa rats compared to control rats at 12 and 19 wk of age. Furthermore, at any age, *in vitro* activities of CS, SDH, and complex IV were similar or increased in fa/fa rats compared to fa/+ rats, pointing toward overall normal functioning of mitochondrial machinery. The *in vitro* data are in agreement with Turner *et al.* (47), who studied various rodent models of high-fat-diet-induced insulin resistance and measured increased activity of medium-chain acylCoA dehydrogenase (another enzyme of the β-oxidation, comparable to VLCAD) and increased activity of CS in fa/fa rats. In addition, they reported increased *in vitro* fatty acid oxidative capacity in muscle homogenates and isolated mitochondria (47). Also, protein expression of peroxisome proliferator-activated receptor γ coactivator (PGC) -1α, a strong activator of mitochondrial biogenesis and oxidative metabolism, and several mitochondrial respiratory chain complexes were found to be up-regulated. Both *in vivo* and *in vitro* data of the present study are in line with these findings, as high IMCL accumulation in fa/fa rats does not seem to be induced by decreased muscle mitochondrial oxidative capacity. In accordance, 8 wk of high-fat diet consumption in Wistar rats resulted in increased IMCL levels but did not affect intrinsic mitochondrial functioning (45).

Genetic models of obesity and insulin resistance are, in general, characterized by an early-established phenotype. The ZDF rat model allows studying the transition from insulin resistance toward overt type 2 diabetes, but not investigation of the mechanisms involved in the development of insulin resistance itself, as the latter is presumably already present in 6-wk-old animals (26). Longitudinal *in vivo* studies of animal models of slowly progressing skeletal muscle insulin resistance are expected to give crucial insights into the role of mitochondrial oxidative capacity in that pathological condition.

Studies in animal models of lipid-induced insulin resistance do not exclude the possibility that an *intrinsic* defect in the skeletal muscle fatty acid oxidative machinery might lead to accumulation of triglycerides and fatty acid metabolites and thereby induce insulin resistance. Dobbins *et al.* (7) showed that inhibiting carnitine palmitoyltransferase-1, thereby blocking the entry of fatty acids into mitochondria, resulted in increased IMCL content, decreased whole-body insulin sensitivity, and decreased glucose disposal in skeletal muscle of

rats. On the other hand, long-chain acyl-CoA dehydrogenase (48) and PGC-1α knockout mice (49) did not show any signs of decreased insulin sensitivity of skeletal muscle tissue. Remarkably, two mouse models characterized by progressive loss of respiratory chain function and activity even showed improved glucose homeostasis and skeletal muscle insulin sensitivity (50, 51). Even more surprisingly, reduced mitochondrial activity made these mice resistant to diabetes and obesity (51). Whether these transgenic mouse models generated compensatory mechanisms protecting them from developing insulin resistance remains to be elucidated.

CONCLUSIONS

We used minimally invasive MRS methods to collect unique longitudinal data of *in vivo* mitochondrial oxidative capacity and IMCL levels in ZDF rats at different stages throughout the development of type 2 diabetes. Despite increased IMCL levels, *in vivo* mitochondrial oxidative capacity did not differ between diabetic and control animals, neither in the prediabetic state nor during full-blown type 2 diabetes. The *in vivo* MRS results were corroborated by *in vitro* enzyme activity data, suggesting even an improved capacity of enzymes involved in fat oxidation in the type 2 diabetic animals. Accordingly, we can conclude that in the ZDF rat model, the transition from insulin resistance to type 2 diabetes does occur in the absence of skeletal muscle mitochondrial dysfunction. FJ

We express our appreciation to Stephan Majoor and Larry de Graaf for their assistance with the *in vivo* experiments and for technical support, respectively. We thank Jos P. N. Ruiter for technical assistance with the enzyme assays and Robin A. de Graaf for help with the implementation of the LASER pulse sequence. M.K.H. is supported by a VIDI grant for innovative research (917.66.359).

REFERENCES

1. DeFronzo, R. A., Jacot, E., Jequier, E., Maeder, E., Wahren, J., and Felber, J. P. (1981) The effect of insulin on the disposal of intravenous glucose. Results from indirect calorimetry and hepatic and femoral venous catheterization. *Diabetes* **30,** 1000–1007
2. Petersen, K. F., and Shulman, G. I. (2006) Etiology of insulin resistance. *Am. J. Med.* **119,** S10–S16
3. Goodpaster, B. H., He, J., Watkins, S., and Kelley, D. E. (2001) Skeletal muscle lipid content and insulin resistance: evidence for a paradox in endurance-trained athletes. *J. Clin. Endocrinol. Metab.* **86,** 5755–5761
4. Krssak, M., Falk Petersen, K., Dresner, A., DiPietro, L., Vogel, S. M., Rothman, D. L., Roden, M., and Shulman, G. I. (1999) Intramyocellular lipid concentrations are correlated with insulin sensitivity in humans: a 1H NMR spectroscopy study. *Diabetologia* **42,** 113–116
5. Pan, D. A., Lillioja, S., Kriketos, A. D., Milner, M. R., Baur, L. A., Bogardus, C., Jenkins, A. B., and Storlien, L. H. (1997) Skeletal muscle triglyceride levels are inversely related to insulin action. *Diabetes* **46,** 983–988
6. Perseghin, G., Scifo, P., De Cobelli, F., Pagliato, E., Battezzati, A., Arcelloni, C., Vanzulli, A., Testolin, G., Pozza, G., Del Maschio, A., and Luzi, L. (1999) Intramyocellular triglyceride content is a determinant of in vivo insulin resistance in humans: a 1H–13C nuclear magnetic resonance spectroscopy assessment in offspring of type 2 diabetic parents. *Diabetes* **48,** 1600–1606
7. Dobbins, R. L., Szczepaniak, L. S., Bentley, B., Esser, V., Myhill, J., and McGarry, J. D. (2001) Prolonged inhibition of muscle carnitine palmitoyltransferase-1 promotes intramyocellular lipid accumulation and insulin resistance in rats. *Diabetes* **50,** 123–130
8. Kuhlmann, J., Neumann-Haefelin, C., Belz, U., Kalisch, J., Juretschke, H. P., Stein, M., Kleinschmidt, E., Kramer, W., and Herling, A. W. (2003) Intramyocellular lipid and insulin resistance: a longitudinal in vivo 1H-spectroscopic study in Zucker diabetic fatty rats. *Diabetes* **52,** 138–144
9. Kuhlmann, J., Neumann-Haefelin, C., Belz, U., Kramer, W., Juretschke, H. P., and Herling, A. W. (2005) Correlation between insulin resistance and intramyocellular lipid levels in rats. *Magn. Reson. Med.* **53,** 1275–1282
10. Shulman, G. I. (2000) Cellular mechanisms of insulin resistance. *J. Clin. Invest.* **106,** 171–176
11. Yu, C., Chen, Y., Cline, G. W., Zhang, D., Zong, H., Wang, Y., Bergeron, R., Kim, J. K., Cushman, S. W., Cooney, G. J., Atcheson, B., White, M. F., Kraegen, E. W., and Shulman, G. I. (2002) Mechanism by which fatty acids inhibit insulin activation of insulin receptor substrate-1 (IRS-1)-associated phosphatidylinositol 3-kinase activity in muscle. *J. Biol. Chem.* **277,** 50230–50236
12. Rabol, R., Boushel, R., and Dela, F. (2006) Mitochondrial oxidative function and type 2 diabetes. *Appl. Physiol. Nutr. Metab.* **31,** 675–683
13. Lowell, B. B., and Shulman, G. I. (2005) Mitochondrial dysfunction and type 2 diabetes. *Science* **307,** 384–387
14. Petersen, K. F., Befroy, D., Dufour, S., Dziura, J., Ariyan, C., Rothman, D. L., DiPietro, L., Cline, G. W., and Shulman, G. I. (2003) Mitochondrial dysfunction in the elderly: possible role in insulin resistance. *Science* **300,** 1140–1142
15. Petersen, K. F., Dufour, S., Befroy, D., Garcia, R., and Shulman, G. I. (2004) Impaired mitochondrial activity in the insulin-resistant offspring of patients with type 2 diabetes. *N. Engl. J. Med.* **350,** 664–671
16. Schrauwen-Hinderling, V. B., Kooi, M. E., Hesselink, M. K., Jeneson, J. A., Backes, W. H., van Echteld, C. J., van Engelshoven, J. M., Mensink, M., and Schrauwen, P. (2007) Impaired in vivo mitochondrial function but similar intramyocellular lipid content in patients with type 2 diabetes mellitus and BMI-matched control subjects. *Diabetologia* **50,** 113–120
17. Befroy, D. E., Petersen, K. F., Dufour, S., Mason, G. F., de Graaf, R. A., Rothman, D. L., and Shulman, G. I. (2007) Impaired mitochondrial substrate oxidation in muscle of insulin-resistant offspring of type 2 diabetic patients. *Diabetes* **56,** 1376–1381
18. Simoneau, J. A., and Kelley, D. E. (1997) Altered glycolytic and oxidative capacities of skeletal muscle contribute to insulin resistance in NIDDM. *J. Appl. Physiol.* **83,** 166–171
19. He, J., Watkins, S., and Kelley, D. E. (2001) Skeletal muscle lipid content and oxidative enzyme activity in relation to muscle fiber type in type 2 diabetes and obesity. *Diabetes* **50,** 817–823
20. Kelley, D. E., He, J., Menshikova, E. V., and Ritov, V. B. (2002) Dysfunction of mitochondria in human skeletal muscle in type 2 diabetes. *Diabetes* **51,** 2944–2950
21. Ritov, V. B., Menshikova, E. V., He, J., Ferrell, R. E., Goodpaster, B. H., and Kelley, D. E. (2005) Deficiency of subsarcolemmal mitochondria in obesity and type 2 diabetes. *Diabetes* **54,** 8–14
22. Mootha, V. K., Lindgren, C. M., Eriksson, K. F., Subramanian, A., Sihag, S., Lehar, J., Puigserver, P., Carlsson, E., Ridderstrale, M., Laurila, E., Houstis, N., Daly, M. J., Patterson, N., Mesirov, J. P., Golub, T. R., Tamayo, P., Spiegelman, B., Lander, E. S., Hirschhorn, J. N., Altshuler, D., and Groop, L. C. (2003) PGC-1alpha-responsive genes involved in oxidative phosphorylation are coordinately downregulated in human diabetes. *Nat. Genet.* **34,** 267–273
23. Patti, M. E., Butte, A. J., Crunkhorn, S., Cusi, K., Berria, R., Kashyap, S., Miyazaki, Y., Kohane, I., Costello, M., Saccone, R., Landaker, E. J., Goldfine, A. B., Mun, E., DeFronzo, R., Finlayson, J., Kahn, C. R., and Mandarino, L. J. (2003) Coordinated reduction of genes of oxidative metabolism in

humans with insulin resistance and diabetes: potential role of PGC1 and NRF1. *Proc. Natl. Acad. Sci. U. S. A.* **100,** 8466–8471
24. Roden, M. (2005) Muscle triglycerides and mitochondrial function: possible mechanisms for the development of type 2 diabetes. *Int. J. Obes. (London)* **29**(Suppl. 2), S111–S115
25. Quistorff, B., Johansen, L., and Sahlin, K. (1993) Absence of phosphocreatine resynthesis in human calf muscle during ischaemic recovery. *Biochem. J.* **291**(Pt. 3), 681–686
26. Etgen, G. J., and Oldham, B. A. (2000) Profiling of Zucker diabetic fatty rats in their progression to the overt diabetic state. *Metabolism* **49,** 684–688
27. De Feyter, H. M., Schaart, G., Hesselink, M. K., Schrauwen, P., Nicolay, K., and Prompers, J. J. (2006) Regional variations in intramyocellular lipid concentration correlate with muscle fiber type distribution in rat tibialis anterior muscle. *Magn. Reson. Med.* **56,** 19–25
28. Garwood, M., and DelaBarre, L. (2001) The return of the frequency sweep: designing adiabatic pulses for contemporary NMR. *J. Magn. Reson.* **153,** 155–177
29. De Graaf, R. A., and Nicolay, K. (1998) Adiabatic water suppression using frequency selective excitation. *Magn. Reson. Med.* **40,** 690–696
30. Vanhamme, L., van den Boogaart, A., and Van Huffel, S. (1997) Improved method for accurate and efficient quantification of MRS data with use of prior knowledge. *J. Magn. Reson.* **129,** 35–43
31. Brindle, K. M., Blackledge, M. J., Challiss, R. A., and Radda, G. K. (1989) 31P NMR magnetization-transfer measurements of ATP turnover during steady-state isometric muscle contraction in the rat hind limb in vivo. *Biochemistry* **28,** 4887–4893
32. Taylor, D. J., Styles, P., Matthews, P. M., Arnold, D. A., Gadian, D. G., Bore, P., and Radda, G. K. (1986) Energetics of human muscle: exercise-induced ATP depletion. *Magn. Reson. Med.* **3,** 44–54
33. Taylor, D. J., Bore, P. J., Styles, P., Gadian, D. G., and Radda, G. K. (1983) Bioenergetics of intact human muscle. A 31P nuclear magnetic resonance study. *Mol. Biol. Med.* **1,** 77–94
34. Lawson, J. W., and Veech, R. L. (1979) Effects of pH and free Mg2+ on the Keq of the creatine kinase reaction and other phosphate hydrolyses and phosphate transfer reactions. *J. Biol. Chem.* **254,** 6528–6537
35. Boska, M. (1994) ATP production rates as a function of force level in the human gastrocnemius/soleus using 31P MRS. *Magn. Reson. Med.* **32,** 1–10
36. Wanders, R. J., Vreken, P., den Boer, M. E., Wijburg, F. A., van Gennip, A. H., and Ijlst, L. (1999) Disorders of mitochondrial fatty acyl-CoA beta-oxidation. *J. Inherit. Metab. Dis.* **22,** 442–487
37. Srere, P. A., Brazil, H., and Gonen, L. (1963) The citrate-condensing enzyme of pigeon breast muscle and moth flight muscle. *Acta Chem. Scand.* **17,** S129–134
38. Munujos, P., Coll-Cantí, J., González-Sastre, F., and Gella, F. J. (1993) Assay of succinate dehydrogenase activity by a colorimetric-continuous method using iodonitrotetrazolium chloride as electron acceptor. *Anal. Biochem.* **212,** 506–509
39. Cooperstein, S. J., and Lazarow, A. (1951) A microspectrophotometric method for the determination of cytochrome oxidase. *J. Biol. Chem.* **189,** 665–670
40. Sanderson, A. L., Kemp, G. J., Thompson, C. H., and Radda, G. K. (1996) Increased oxidative and delayed glycogenolytic ATP synthesis in exercising skeletal muscle of obese (insulin-resistant) Zucker rats. *Clin. Sci. (London)* **91,** 691–702
41. Klein, M., Kaminsky, P., Walker, P. M., Straczek, J., Barbe, F., Duc, M., and Burlet, C. (1994) Muscle bioenergetics in obese Zucker rats. *Am. J. Physiol.* **266,** E410–E417
42. Chanseaume, E., Tardy, A. L., Salles, J., Giraudet, C., Rousset, P., Tissandier, A., Boirie, Y., and Morio, B. (2007) Chronological approach of diet-induced alterations in muscle mitochondrial functions in rats. *Obesity (Silver Spring)* **15,** 50–59
43. Iossa, S., Mollica, M. P., Lionetti, L., Crescenzo, R., Botta, M., and Liverini, G. (2002) Skeletal muscle oxidative capacity in rats fed high-fat diet. *Int. J. Obes. Relat. Metab. Disord.* **26,** 65–72
44. Lionetti, L., Mollica, M. P., Crescenzo, R., D'Andrea, E., Ferraro, M., Bianco, F., Liverini, G., and Iossa, S. (2007) Skeletal muscle subsarcolemmal mitochondrial dysfunction in high-fat fed rats exhibiting impaired glucose homeostasis. *Int. J. Obes. (London)* **31,** 1596–1604
45. Hoeks, J., Briede, J. J., de Vogel, J., Schaart, G., Nabben, M., Moonen-Kornips, E., Hesselink, M. K. C., and Schrauwen, P. (2008) Mitochondrial function, content and ROS production in rat skeletal muscle: effect of high-fat feeding. *FEBS Lett.* **582,** 510–516
46. Bonnard, C., Durand, A., and Chauvin, M. A. (2008) Mitochondrial dysfunction results from oxidative stress in the skeletal muscle of diet-induced insulin-resistant mice. *J. Clin. Invest.* **118,** 789–800
47. Turner, N., Bruce, C. R., Beale, S. M., Hoehn, K. L., So, T., Rolph, M. S., and Cooney, G. J. (2007) Excess lipid availability increases mitochondrial fatty acid oxidative capacity in muscle: evidence against a role for reduced fatty acid oxidation in lipid-induced insulin resistance in rodents. *Diabetes* **56,** 2085–2092
48. Zhang, D., Liu, Z. X., Choi, C. S., Tian, L., Kibbey, R., Dong, J., Cline, G. W., Wood, P. A., and Shulman, G. I. (2007) Mitochondrial dysfunction due to long-chain Acyl-CoA dehydrogenase deficiency causes hepatic steatosis and hepatic insulin resistance. *Proc. Natl. Acad. Sci. U. S. A.* **104,** 17075–17080
49. Handschin, C., Choi, C. S., Chin, S., Kim, S., Kawamori, D., Kurpad, A. J., Neubauer, N., Hu, J., Mootha, V. K., Kim, Y. B., Kulkarni, R. N., Shulman, G. I., and Spiegelman, B. M. (2007) Abnormal glucose homeostasis in skeletal muscle-specific PGC-1alpha knockout mice reveals skeletal muscle-pancreatic beta cell crosstalk. *J. Clin. Invest.* **117,** 3463–3474
50. Wredenberg, A., Freyer, C., Sandstrom, M. E., Katz, A., Wibom, R., Westerblad, H., and Larsson, N. G. (2006) Respiratory chain dysfunction in skeletal muscle does not cause insulin resistance. *Biochem. Biophys. Res. Commun.* **350,** 202–207
51. Pospisilik, J. A., Knauf, C., Joza, N., Benit, P., Orthofer, M., Cani, P. D., Ebersberger, I., Nakashima, T., Sarao, R., Neely, G., Esterbauer, H., Kozlov, A., Kahn, C. R., Kroemer, G., Rustin, P., Burcelin, R., and Penninger, J. M. (2007) Targeted deletion of AIF decreases mitochondrial oxidative phosphorylation and protects from obesity and diabetes. *Cell* **131,** 476–491

Received for publication April 30, 2008.
Accepted for publication June 26, 2008.